



1994 Summary Report for ITER Design Task D4.
*Shielding 3D Analysis. Afterheat Analysis
for the Whole Machine and Cryostat Area.*
Part A: Neutronics and Shielding

M.E. Sawan, L.A. El-Guebaly, H.Y. Khater

January 1995

UWFDM-976

FUSION TECHNOLOGY INSTITUTE
UNIVERSITY OF WISCONSIN
MADISON WISCONSIN

DISCLAIMER

This report was prepared as an account of work sponsored by an agency of the United States Government. Neither the United States Government, nor any agency thereof, nor any of their employees, makes any warranty, express or implied, or assumes any legal liability or responsibility for the accuracy, completeness, or usefulness of any information, apparatus, product, or process disclosed, or represents that its use would not infringe privately owned rights. Reference herein to any specific commercial product, process, or service by trade name, trademark, manufacturer, or otherwise, does not necessarily constitute or imply its endorsement, recommendation, or favoring by the United States Government or any agency thereof. The views and opinions of authors expressed herein do not necessarily state or reflect those of the United States Government or any agency thereof.

1994 Summary Report for ITER Design Task D4

**Shielding 3D Analysis. Afterheat Analysis for the
Whole Machine and Cryostat Area**

Part A: Neutronics and Shielding

M. E. Sawan, L. A. El-Guebaly, and H. Y. Khater

Fusion Technology Institute
University of Wisconsin-Madison
1500 Johnson Drive
Madison, WI 53706

January 1995

UWFDM-976

Executive Summary

This design task is aimed at modeling the ITER reactor for three-dimensional Monte Carlo, determining the neutron wall loading distribution, performing preliminary three-dimensional shielding calculations for the divertor region and performing activation calculations. Due to the continuously evolving design over the year, most of the analysis was performed for the ITER outline design. An effort started to model the most recent divertor cassette design presented at the end of October in the design assessment meeting. A revised 3D model of ITER was developed with the new divertor cassette design. Because of delays in the ITER design activities it was necessary during the year to respond to requests from the JCT to provide support in the neutronics area. This report summarizes the work performed and the results obtained in this design task during the year 1994.

A source subroutine was written to modify the 3D Monte Carlo neutronics code MCNP to sample source neutrons from the source distribution in ITER plasma. A general ITER 3D model for MCNP was developed jointly by the US and EU home teams and submitted along with the source term to the Garching JCT in March as required by the task milestones. The model is based on the ITER outline design. The model includes the detailed configurations of the first wall, blanket, divertor, vacuum vessel and TF magnets. The model also includes the pumping slots in the outer leg of the divertor. The poloidal distribution of the neutron wall loading in the different regions of the ITER outline design has been determined using the Monte Carlo code MCNP. The average neutron wall loading is 0.913 MW/m^2 for the nominal 1500 MW fusion power. The calculated average neutron wall loadings at the outboard and inboard first wall, are 1.044 and 0.735 MW/m^2 , respectively. The peak outboard and inboard neutron wall loadings are 1.193 and 0.923 MW/m^2 , respectively.

Detailed 3D neutronics calculations have been performed for the divertor region in the outline design. The walls of the horizontal ducts are completely out of the direct line of sight of source neutrons. The ducts are shielded from the plasma region by the approximately 80 cm thick lower end of the outboard blanket/shield and by the 40-60 cm thick outer divertor leg in front of the lower half of the duct. Based on this analysis, it is concluded that no additional divertor duct shielding will be needed and the 20 cm thick duct wall along with the 11 cm thick mechanical structure will provide adequate protection for the TF coils against streaming radiation. In addition, parts of the TF coils behind the divertor cassettes are well shielded. Preliminary estimates of total nuclear heating in the TF coils were determined for both the SS/water and Li/V blankets of the ITER outline design. The results were based on the 3D calculations performed for the outline design. The total heating is less than 5 kW. The total heating is increased to 7 kW for the recent shielding blanket design presented in October at the design assessment meeting.

Detailed activation analysis has been performed for the first wall/blanket/vacuum vessel/magnet in the ITER outline design using different pulsed operation schedules. The calculations were performed for both the shielding blanket (SS/water) and the breeding blanket (Li/V) options. The activation code RACC modified for pulsing operation was used in the calculations. The detailed activation results include the spatial distribution of the radioactive inventory, afterheat and contact dose at different times following shutdown.

The nuclear performance parameters for the first wall/blanket/vacuum vessel/magnet in the ITER outline design were determined using data based on the FENDL evaluation and compared to those obtained with previously used cross section libraries based on the ENDF/B-V evaluation. The calculations were performed for both the shielding blanket (SS/water) and the breeding blanket (Li/V) options. The detailed neutronics and shielding results were provided to the ITER JCT. A working multigroup cross section library based on the most recent international fusion evaluated nuclear data library (FENDL) was generated. The library includes all nuclear responses of interest for the ITER design. The library was installed on the Garching JWS computer system in September. Neutronics, shielding, and activation benchmark problems have been developed based on the shielding blanket design in the ITER outline design. The specifications and required neutron flux files were provided to the neutronics groups of the home teams. Results will help the JCT determine the codes and libraries to be used in neutronics, shielding and activation calculations.

The neutron source profile and plasma shape have not changed from the outline design. The major changes are in the divertor cassette design. In addition to the significant geometrical configuration changes, each divertor cassette includes 28 slots compared to only 5 slots in the outline design. The design presented at the end of October in the design assessment meeting was used as the basis for the updated general reactor 3D model. A complete updated general reactor model is provided to replace the model provided in March. Although more divertor slots are used, streaming through the horizontal divertor ports is expected to be lower than in the outline design since these slots are not directed towards the horizontal ports. On the other hand, these slots can result in damage hot spots in the vacuum vessel behind the divertor cassettes. This effect needs to be investigated. It is assumed that the geometrical configurations for the first wall, blanket, vacuum vessel and magnets are the same as in the previous model based on the outline design. It is expected that the designs for these components will go through several changes and the 3D model has to be updated again in 1995.

I. Introduction

An outline design for ITER has been developed during the first eighteen months of the ITER EDA [1]. Due to the continuously changing design over the year, most of the analysis in this task was performed for the ITER outline design. Significant poloidal variation in neutron wall loading is expected in ITER. The neutron wall loading distribution is an essential input for neutronics analysis of the different ITER components. The detailed poloidal distribution of the neutron wall loading in the different regions of ITER was determined using the Monte Carlo code MCNP [2].

The ITER outline design provides a nominal fusion power of 1.5 GW from a single null plasma. Twenty-four toroidal field (TF) coils are employed. The design incorporates an advanced divertor concept at the bottom of the reactor. The vacuum vessel (VV) is a double wall structure that acts as a shielding component and containment structure. 24 large lower ports are utilized for assembly and disassembly of the divertor cassettes and for vacuum pumping. Radiation streaming into these ports can produce excessive heating and damage the TF coils in the divertor region. Reducing nuclear heating in the TF coils to acceptable levels has been identified as an important shielding issue. The peak magnet radiation effects as well as the integrated nuclear heating have been calculated in the parts of the coils adjacent to the vacuum pumping ducts using MCNP. The total nuclear heating in the TF coils of ITER has been determined taking into account the poloidal variation of the neutron wall loading as well as the poloidal variation of the blanket/shield/vacuum vessel thickness. The results of the three-dimensional neutronics analysis are summarized here.

In order to ensure consistent neutronics analyses for the different ITER components, it was decided that a general three-dimensional geometrical model for ITER should be developed for the MCNP code and made available to the JCT and home teams. The model explained in this report was developed jointly by the US and EU home teams and submitted along with the source term to the JCT and home teams. An effort started in the US to model the most recent divertor cassette design presented at the end of October 1994 in the design assessment meeting. A complete updated general reactor model is provided to replace the model provided in March.

Detailed activation analysis has been performed for the first wall/blanket/vacuum vessel/magnet in the ITER outline design using different pulsed operation schedules. The calculations were performed for both the shielding blanket (SS/water) and the breeding blanket (Li/V) options. The activation code RACC modified for pulsed operation was used in the calculations. The detailed activation results are given in a separate report [3]. The results include the detailed spatial distribution of the radioactive inventory, afterheat and contact dose at different times following shutdown. This information is needed for safety analysis, radwaste management and maintenance assessment.

Because of the continuously evolving ITER design, it was necessary during the year to respond to requests from the JCT to provide support in the neutronics area. A working cross section library based on the most recent international fusion evaluated nuclear data library (FENDL) [4] was generated and installed on the Garching JWS computer system in September. In addition, the nuclear performance parameters for the first wall/blanket/vacuum vessel/magnet in the ITER outline design were determined using data based on the FENDL evaluation and compared to those obtained with previously used cross section libraries based on the ENDF/B-V evaluation. The calculations were performed for both the shielding blanket (SS/water) and the breeding blanket (Li/V) options. The neutronics and shielding results are summarized in this report. Neutronics, shielding, and activation benchmark problems have been developed based on the shielding blanket design in the ITER outline design. The specifications and required flux files were provided to the neutronics groups of the home teams. The results will help the JCT determine the codes and libraries to be used in neutronics, shielding and activation calculations.

II. Neutron Wall Loading Distribution

The poloidal distribution of the neutron wall loading in the different regions of ITER has been determined using the three-dimensional radiation transport Monte Carlo code MCNP [2]. The results are normalized to the nominal fusion power of 1500 MW. The detailed geometrical configuration of the ITER first wall has been modeled in the calculation. An output of the MCNP geometry plotting routine is given in Fig. 1. It shows a vertical cross section of the geometrical model used in the calculations. A combination of cones, tori, and cylinders was utilized for accurate modeling of the first wall. Source neutrons are sampled from the plasma zone according to the source distribution within the single null plasma shape. The radial and vertical shifts of the magnetic axis where the fusion power density peaks have been taken into account. The magnetic axis is located at a radius of 8.633 m and is 1.622 m above the reactor midplane. The direction of source particles has been sampled from an isotropic angular distribution. Three million source particles have been sampled in the MCNP calculation yielding statistical uncertainty less than 0.5 % in the calculated wall loading at any first wall segment.

Source particles travel through void in the plasma chamber until they cross the wall. Particles are killed upon crossing the wall to account for the shadowing effect. Surface current tallies have been determined by counting particles crossing the wall. These current tallies represent the neutron wall loading. In order to get the detailed poloidal distribution of the neutron wall loading, the first wall surface has been segmented into 106 poloidal segments and particles crossing each segment have been tallied. The outboard and inboard first wall surface areas are 800 and 421 m², respectively, and the area at the entrance to the divertor region is 94 m². Therefore, the average neutron wall loading is 0.913 MW/m² for the nominal 1500 MW fusion power. The calculated

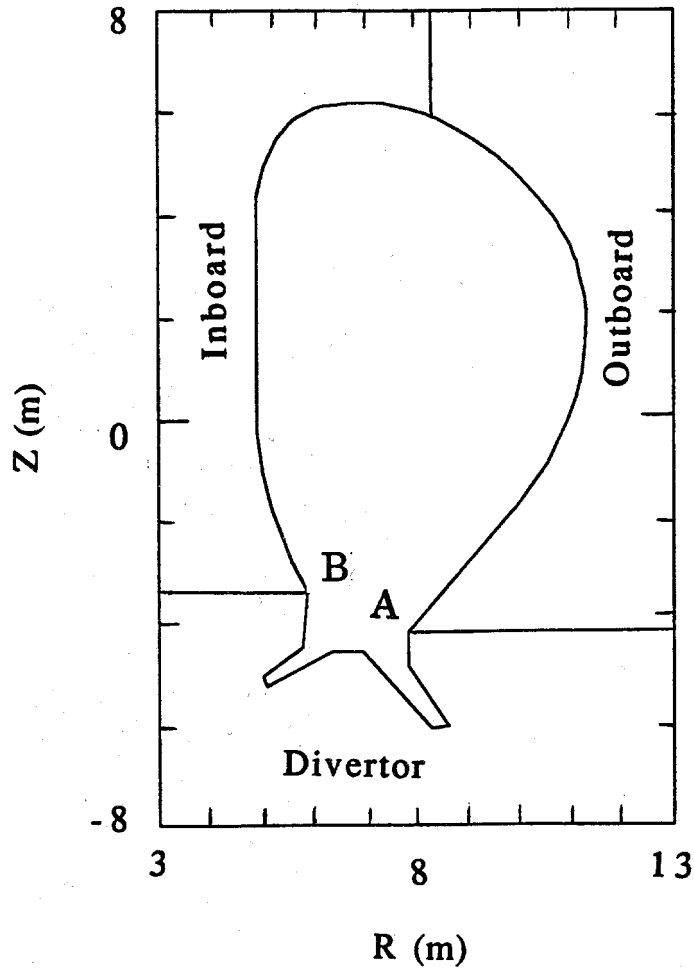


Fig. 1. The ITER first wall geometrical model used in the MCNP calculations.

average neutron wall loadings at the outboard first wall, inboard first wall, and entrance to the divertor region are 1.044, 0.735, and 0.6 MW/m², respectively. The total area of surfaces exposed to the plasma in the divertor region is 372 m² with an average neutron wall loading of 0.148 MW/m².

Figure 2 gives the poloidal variation of neutron wall loading in the outboard and inboard regions as a function of toroidal length measured in the anticlockwise direction from the lower corner of the outboard first wall (point A in Fig. 1). The peak outboard and inboard neutron wall loadings are 1.193 and 0.923 MW/m², respectively. It is clear that the neutron wall loading peaks at vertical locations close to that of the plasma magnetic axis. Figure 3 shows the poloidal variation of neutron wall loading in the divertor region as a function of length measured in the anticlockwise direction from the upper left corner of the divertor region (point B in Fig. 1). The peak neutron

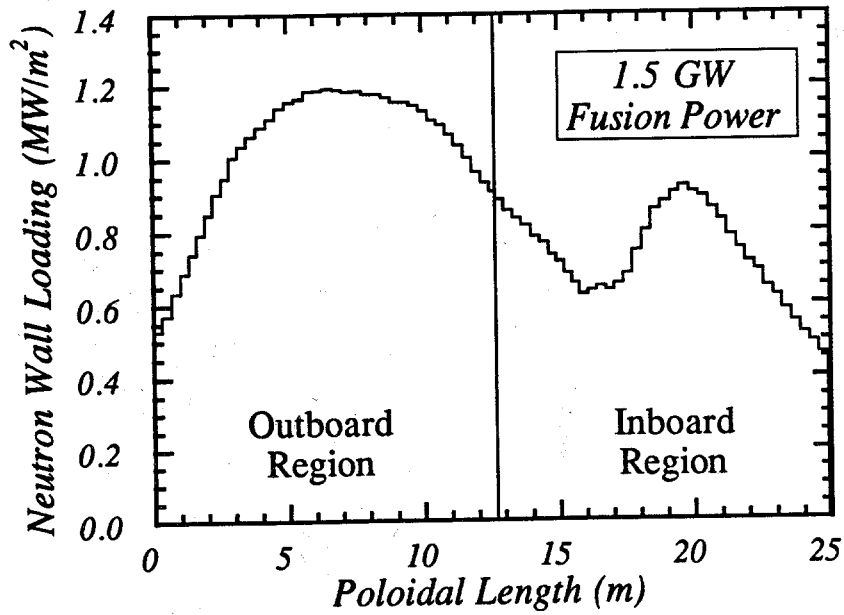


Fig. 2. The poloidal variation of neutron wall loading in the outboard and inboard regions as a function of toroidal length.

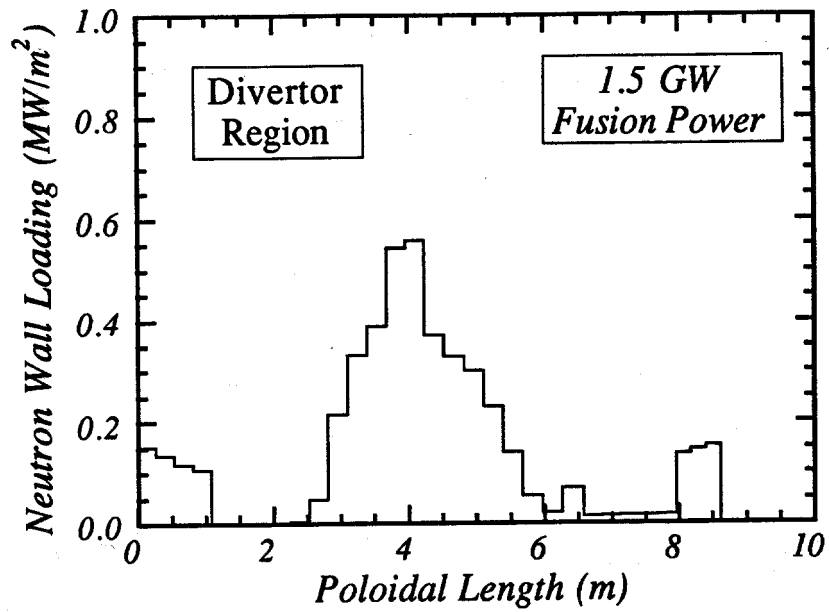


Fig. 3. The poloidal variation of neutron wall loading in the divertor region as a function of toroidal length.

Table 1. Neutron Wall Loading in ITER

Average Neutron Wall Loading	0.913 MW/m ²
Outboard Region:	
Surface Area	800 m ²
Average Neutron Wall Loading	1.044 MW/m ²
Peak Neutron Wall Loading	1.193 MW/m ²
Inboard Region:	
Surface Area	421 m ²
Average Neutron Wall Loading	0.735 MW/m ²
Peak Neutron Wall Loading	0.923 MW/m ²
Divertor Region:	
Surface Area	372 m ²
Average Neutron Wall Loading	0.148 MW/m ²
Peak Neutron Wall Loading	0.559 MW/m ²

wall loading in the divertor region is 0.559 MW/m² at the upper surface of the middle divertor plate facing the plasma x-point. No direct source neutrons impinge on the inner surface of the inner divertor leg. The average neutron wall loading at the inner surface of the outer divertor leg is only 0.016 MW/m². The values of neutron wall loading at the inner and outer divertor dump plates with the least magnet shielding space are 0.0009 and 0.07 MW/m², respectively. Table 1 summarizes the results of the neutron wall loading calculations for the nominal 1500 MW fusion power. During the plasma power excursions of 1800 MW fusion power, these values will be 20% higher.

The detailed neutron wall loading results obtained by MCNP were provided to the EU home team for comparison with the results generated using the TRIPOLI Monte Carlo code [5]. Some discrepancies were observed in the results with differences up to 12% [6]. These discrepancies are mainly due to differences in geometrical modelling. While the MCNP model given here follows the exact representation of the ITER first wall, the TRIPOLI modelling is less accurate for the first wall and uses a smaller number of mesh points (24x35) to represent the source [6].

III. Three-Dimensional Shielding Analysis for the Divertor Region

Providing adequate protection for the TF coils against radiation streaming into the divertor vacuum pumping ducts has been identified as an important shielding issue for the current ITER design. Due to the geometrical complexity of the divertor region, three-dimensional models are required to properly determine the radiation effects in the parts of the TF coils adjacent to the divertor vacuum pumping duct. Furthermore, the parts of the TF coils behind the divertor are protected from source neutrons by the divertor modules and the vacuum vessel with varying

thickness and geometrical shape. Magnet hot spots are expected behind the inner and outer divertor dump plates where the shielding space is minimal. At these locations the combined thickness of the divertor and vacuum vessel is only about 90 cm. Again, three-dimensional calculations are needed to determine magnet damage in these zones.

Three-dimensional neutron-gamma transport calculations have been performed for magnet shielding in the divertor region taking into account streaming into the divertor vacuum pumping ducts. The continuous energy, coupled neutron-gamma-ray Monte Carlo code MCNP [2] has been used. The nuclear data used is based on the ENDF/B-V evaluation. A three-dimensional model has been developed for the ITER reactor to be used with the MCNP code. The model is based on the ITER outline design [1].

The detailed geometrical configuration of the first wall, blanket, shield, vacuum vessel, divertor and TF coils in the current ITER design has been modeled in the calculation. Several additional surfaces have been added in the divertor region to allow for utilizing the geometry splitting with Russian Roulette variance reduction techniques employed in MCNP. Due to symmetry, only 1/48 of the reactor is modeled with surrounding reflecting boundaries. The model includes half a TF coil and half a divertor duct. The toroidal angle for the model used is 7.5 degrees.

The output of the MCNP geometry plotting routine given in Fig. 4 shows a vertical cross section through the middle of the TF coil. This cross section cuts through one of the pumping slots in the outer leg of the divertor. There are five such slots in each of the 24 divertor modules. The TF magnet in the divertor region is divided into five zones as indicated in Fig. 4. The first zone is behind the inner divertor dump plate, the second zone is behind the inner part of the divertor, the third zone is behind the outer part of the divertor, the fourth zone is behind the outer divertor dump plate, and the fifth zone is adjacent to the divertor vacuum pumping duct. A vertical cross section through the center of the divertor duct is shown in Fig. 5. Fig. 6 is a horizontal cross section at $z = -5.5$ m in the middle of the divertor vacuum pumping duct. The divertor pumping slots in the outer leg of the divertor are shown in this figure. Also shown are the shielding layers between the duct and the coil consisting of the 3 cm thick front Inconel wall, the 14 cm thick steel/water zone, and the 3 cm thick back Inconel wall of the duct wall as well as the 11 cm thick mechanical structure.

A combination of cones, tori, cylinders, and planes was utilized for accurate modeling of the geometry. A total of 147 surfaces has been used in the model, of which 32 are fourth degree tori and 58 are cones. The model employs 119 geometrical cells. The volumes of the different cells and the areas of surfaces of interest have been determined stochastically by ray tracing. In this calculation, all cells are assumed to not include any material and the geometrical model has been

sprayed by 10 million particles at random directions. This calculation serves also as a means for geometry checking by making sure that each point in space belongs to one of the cells used in the model. This calculation provided a successful check for the geometrical model.

The MCNP code has been modified to sample source neutrons from the plasma zone according to the source distribution, provided by the ITER JCT team, with the single null plasma shape as explained in the previous section. Source neutrons are biased to improve the statistical uncertainty in the calculated magnet responses in the divertor region. Surface flux tallies are used to determine the radiation effects at the front and side surfaces of the TF coils in the divertor region and cell energy deposition tallies are used to determine the total magnet heating in the five magnet zones used in the divertor region.

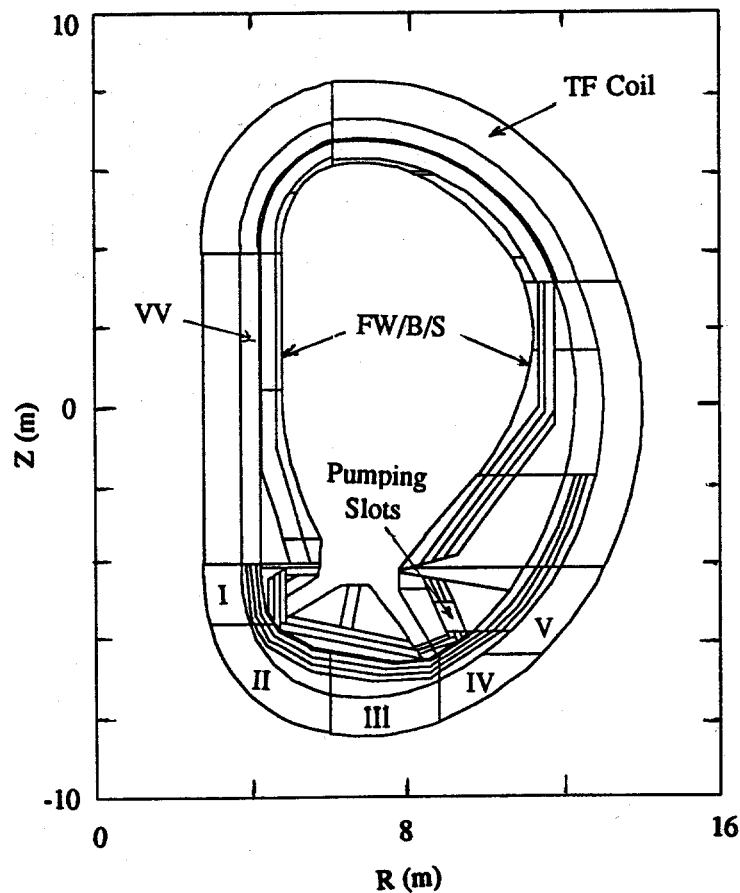


Fig. 4. A vertical cross section through the middle of the TF coil.

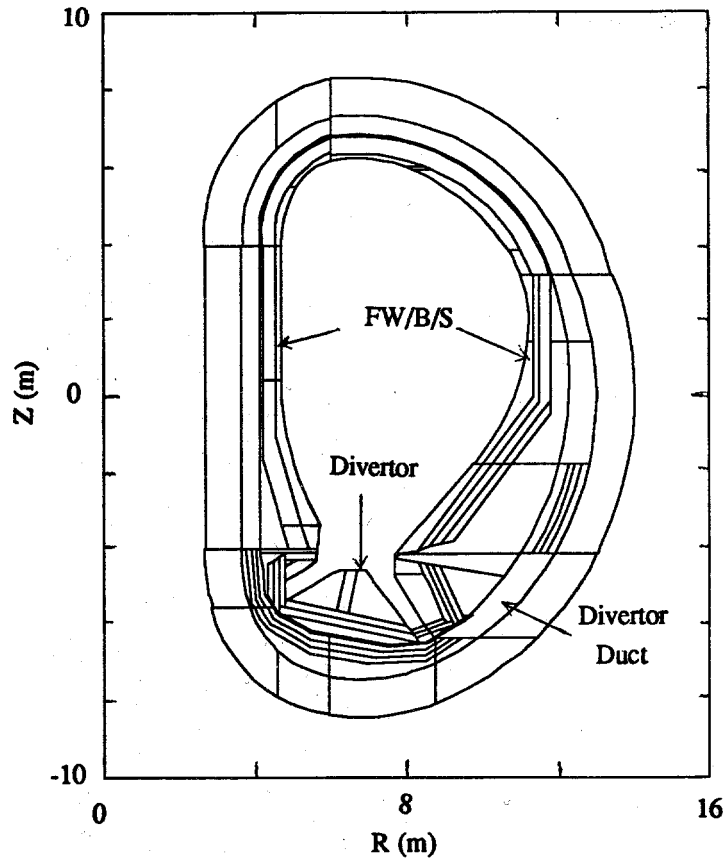


Fig. 5. A vertical cross section through the center of the divertor duct.

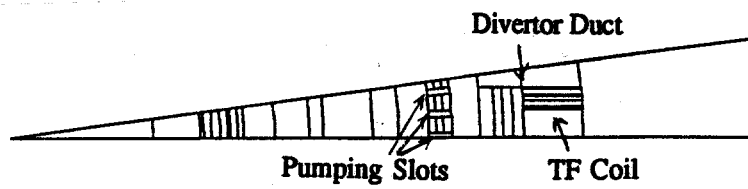


Fig. 6. A horizontal cross section at the middle of the divertor vacuum pumping duct.

In this calculation, it is assumed that no additional divertor duct shielding is utilized and magnet protection is provided by the 20 cm thick duct wall along with the 11 cm thick mechanical structure. No credit is taken for the additional shielding provided by the divertor coolant supply lines inside the duct. In addition, no credit is taken for the fins and support structure at the inner surfaces of the divertor legs that provide additional radiation attenuation. However, the model developed for MCNP calculations includes cells representing the zones where these fins and their support structure can be included. Although this calculation assumes void in these cells, structural material with the appropriate density factor can be used in these cells in the future to assess the impact on magnet shielding. Different material compositions are assumed for the different cells used in the model. The blanket is assumed to consist of 70% 316 SS and 30% water. The vacuum vessel composition used includes 12% Inconel 625, 55% 316 SS and 33% water. The filling material for the duct wall is 60% 316 SS and 40% water. The mechanical structure at the sides of the magnets is made of 316 SS and the divertor module consists of 70% 316 SS and 30% water. The TF coil composition used in the calculation is 31.6% SS, 26% Cu, 9.5% non-Cu (2.5% Nb₃Sn, 6.4% Bronze, 0.6% V), 21.1% liquid He, and 11.8% insulator (epoxy with 70% R-glass).

The calculation has been performed using 200,000 source particles yielding statistical uncertainties less than 10% in the calculated magnet nuclear responses at the locations of interest. The results are normalized to the nominal fusion power of 1500 MW. The end of life fluence related radiation effects have been determined for 3 full power years (FPY) of operation.

Table 2 gives the magnet radiation effects in the part of the TF coil adjacent to the divertor vacuum pumping duct (zone V in Fig. 4). The results are given at the front and side surfaces of the coil. It is clear that the sides of the TF coils are well protected from radiation streaming into the divertor vacuum pumping ducts. The contribution to total magnet heating from the parts of the coils adjacent to the divertor ducts is only 0.21 kW.

Table 3 gives the magnet radiation effects averaged over the front surface of the TF coil in zones I, II, III, and IV shown in Fig. 4. The largest magnet radiation effects are in zone IV behind the outer divertor dump plates where the shielding space is minimal. Although the shielding space behind the inner divertor dump plates is smaller, the magnet radiation effects in zone I are lower than those in zone IV since the inner divertor dump plates have a direct view of a smaller part of the plasma with lower power density. The values of neutron wall loading at the inner and outer divertor dump plates are 0.0009 and 0.07 MW/m², respectively. It should be noted that the radiation effects in the magnet zones I to IV calculated here are conservative since no credit is taken for attenuation in the divertor fins and their support structure, the mechanical structure at the sides

**Table 2. Magnet Radiation Effects at the Front and Side Surfaces
of the TF Coils Adjacent to the Divertor Duct**

	Front Surface	Side Surface
End-of-Life Organic Insulator Dose (Rads @ 3 FPY)	1.50×10^7	3.53×10^7
End-of Life Fast Neutron Fluence in Magnet (n/cm ² @ 3 FPY)	8.22×10^{15}	4.14×10^{16}
End-of-Life Cu dpa in Magnet (dpa @ 3 FPY)	4.11×10^{-6}	1.82×10^{-5}
Specific Nuclear Heating in Magnet (mW/cm ³)	0.0084	0.014

**Table 3. Magnet Radiation Effects at the Front Surface
of the TF Coil Behind the Divertor**

Zone	I	II	III	IV
End-of-Life Organic Insulator Dose (Rads @ 3 FPY)	1.69×10^7	2.44×10^6	1.62×10^6	4.04×10^7
End-of Life Fast Neutron Fluence in Magnet (n/cm ² @ 3 FPY)	7.11×10^{15}	9.93×10^{15}	5.10×10^{14}	2.90×10^{16}
End-of-Life Cu dpa in Magnet (dpa @ 3 FPY)	7.83×10^{-6}	7.26×10^{-7}	2.31×10^{-7}	1.82×10^{-5}
Specific Nuclear Heating in Magnet (mW/cm ³)	0.0081	0.0047	0.0011	0.018

of the coils, and the lower wall of the divertor duct. The calculated radiation effects are much lower than the radiation limits considered in ITER.

IV. Total Nuclear Heating in the TF Coils

The contributions to total magnet heating from the parts of the coils in the divertor region are 0.034, 0.0063, 0.046, 0.87, and 0.21 kW, in zones I, II, III, IV, and V, respectively. The total heating in the 24 TF coils contributed by the divertor region is 1.17 kW. The parts of the TF coils behind the divertor are protected from source neutrons by the divertor modules and the vacuum vessel. The smallest shielding space is behind the inner and outer divertor dump plates as shown

in Fig. 4. At these locations the combined thickness of the divertor and vacuum vessel is 96 cm. The thickness increases rapidly as one moves away from the dump plates reaching 250 cm at the middle of the divertor where the neutron wall loading peaks at 0.56 MW/m^2 . Hence, magnet heating behind the divertor is dominated by heating in the areas behind the divertor dump plates. Nuclear heating in the parts of the magnets adjacent to the divertor vacuum pumping ducts has been determined to be only 0.21 kW. This assumes that no separate duct shield is used.

The parts of the TF coils behind the upper and the middle straight segments of the inboard blanket have a combined blanket/shield/vacuum vessel thickness of 100 cm between them and the plasma and an average neutron wall loading of 0.783 MW/m^2 . One-dimensional calculations have been performed for these sections to determine the nuclear heating per meter length of the TF coils. The calculations have been performed using the discrete ordinates code ONEDANT [7] for both the 316SS/water shielding blanket and the Li/V breeding blanket options considered in the ITER outline design. For 1 MW/m^2 neutron wall loading, the results are 0.196 and 0.239 kW/m for the SS/water and Li/V options, respectively. Based on these results the values for total magnet heating in the parts of the TF coils behind the upper and the middle straight segments of the inboard blanket are 1.26 and 1.53 kW for the SS/water and Li/V options, respectively. The lower curved portion of the inboard blanket increases in thickness as one moves towards the lower tip of it as shown in Fig. 4. In addition, the neutron wall loading drops from 0.83 MW/m^2 at the upper end of this blanket segment to 0.46 MW/m^2 at the lower tip. An appropriate integration procedure, that takes into account the variation of both the neutron wall loading and the blanket/shield/vacuum vessel thickness, has been utilized to determine nuclear heating in the parts of the TF coils behind this blanket segment. This yields 0.08 and 0.1 kW for the SS/water and Li/V options, respectively.

The parts of the TF coils behind the upper segment of the outboard blanket have a combined blanket/shield/vacuum vessel thickness of 100 cm between them and the plasma and an average neutron wall loading of 1.141 MW/m^2 . The values for total magnet heating in these parts of the TF coils have been determined to be 1.33 and 1.63 kW for the SS/water and Li/V options, respectively. The lower segment of the outboard blanket as well as the part of the vacuum vessel behind it increase in thickness as one moves towards the lower tip of it as shown in Fig. 4. In addition, the neutron wall loading drops from 1.193 MW/m^2 at the upper end of this blanket segment to 0.531 MW/m^2 at the lower tip. An integration procedure was utilized yielding 0.3 and 0.36 kW for the SS/water and Li/V options, respectively. Table 4 gives the magnet nuclear heating in the different reactor regions for both the 316SS/water shielding blanket and the Li/V breeding blanket designs. The values for the total nuclear heating in the 24 TF coils are 4.14 and 4.79 kW for the SS/water and Li/V options, respectively. One-dimensional neutronics calculations for the most recent shielding blanket design, presented at the design assessment meeting in October 1994,

Table 4. Total Nuclear Heating (kW) in the TF Coils of ITER

	316SS/Water Shielding Blanket	Li/V Breeding Blanket
Inboard Region	1.34	1.63
Outboard Region	1.63	1.99
Divertor Region	1.17	1.17
Total	4.14	4.79

indicated that local magnet radiation effects in the inboard and outboard regions are a factor of two higher than those for the shielding blanket in the outline design. Therefore, the total magnet heating with the most recent shielding blanket design is estimated to be about 7 kW. All these values do not include any safety factor.

V. General Reactor Model and Source Term for the Outline Design

For consistency of neutronics analyses, a general three-dimensional geometrical model for ITER was developed jointly by the US and EU home teams for the MCNP code. The model was submitted to the Garching JCT in March for distribution to the home teams involved in neutronics design tasks. The model is based on the ITER outline design. Due to symmetry, only 1/48 of the reactor was modeled with surrounding reflecting boundaries. The model includes half a TF coil and half a divertor cassette. The toroidal angle for the model used is 7.5 degrees. A combination of cones, tori, cylinders, and planes was utilized for accurate modeling of the geometry. A total of 197 surfaces and 167 geometrical cells has been used in the model. The model includes detailed geometrical representation of the first wall, blanket, divertor, vacuum vessel and TF magnets. The Be coating and the Cu layer of the first wall are modeled separately. The double walls of the vacuum vessel as well as the shield layer at the back of the vacuum vessel are included in the model. The pumping slots in the outer leg of the divertor are also included. There are 5 such slots per divertor cassette. The output of the MCNP geometry plotting routine given in Fig. 7 shows a vertical cross section through the TF coil. Figure 8 shows a horizontal cross section through the divertor pumping slots.

A source subroutine has been written to modify MCNP to sample source neutrons from the source distribution in the ITER single null plasma. The source profile was provided numerically by the San Diego JCT at 15251 (101×151) mesh points. The source distribution takes into account the radial and vertical shifts of the magnetic axis where the fusion power density peaks. The magnetic axis is located at a radius of 8.633 m and is 1.622 m above the reactor midplane. The direction of source particles is sampled from an isotropic angular distribution. The source

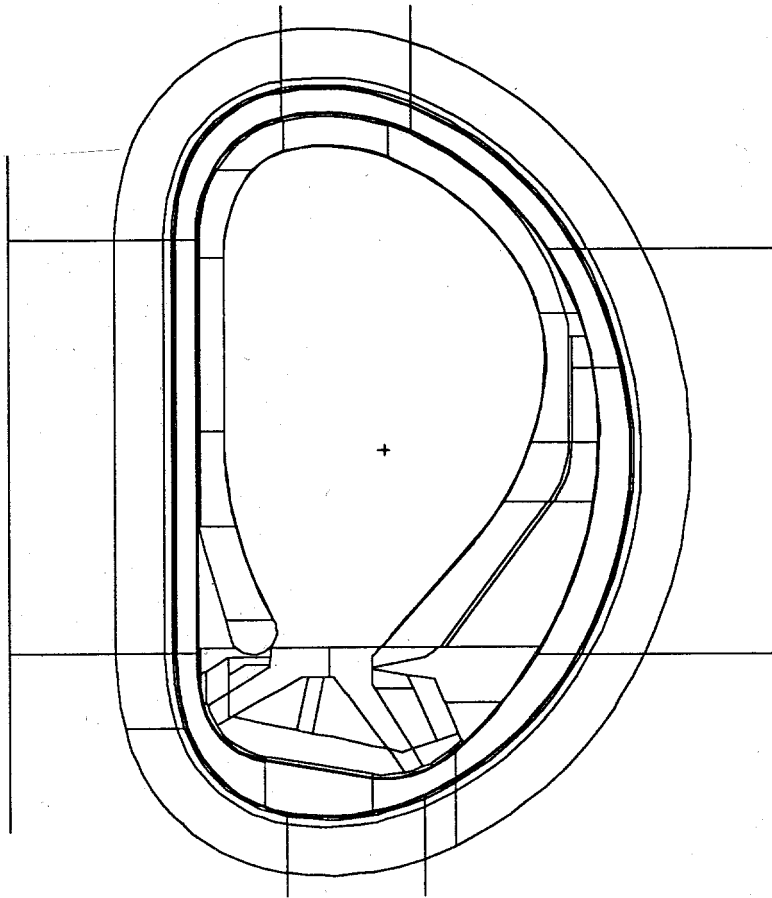


Fig. 7. Vertical cross section through a TF coil.

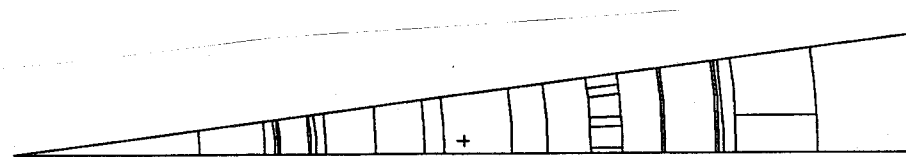


Fig. 8. Horizontal cross section through divertor pumping slots.

subroutine with the associated data files that describe the source distribution were made available to the JCT and home teams.

VI. Revised General Reactor Model With New Divertor Cassette Design

The neutron source profile and plasma shape have not changed from the outline design. The major changes are in the divertor cassette design. In addition to the significant geometrical configuration changes, each divertor cassette includes seven sets of slots with each set including four slots arranged toroidally. Some of these slots will be empty and used for vacuum pumping while the others are employed to house the coolant pipes. Two sets of slots are located behind the outer target plates and two sets are behind the inner target plates. A set of slots also exists behind the central dome. The two main sets of vacuum pumping slots are located in the middle part of the divertor cassette compared to the 5 slots in the outer divertor legs used in the outline design modeled in Fig. 8. Although the divertor design is continuously changing, the design presented at the end of October 1994 in the design assessment meeting was used as the basis for the updated general reactor 3D model. A drawing of this most recent divertor cassette design is given in Fig. 9.

A complete updated general reactor model was developed to include the most recent divertor cassette design. Only 1/48 of the reactor was modeled with surrounding reflecting boundaries. The model includes half a TF coil and half a divertor cassette. The toroidal angle for the model used is 7.5 degrees. A combination of cones, tori, cylinders, and planes was utilized for accurate modeling of the geometry. A total of 216 surfaces and 172 geometrical cells has been used in the model. It is assumed that the geometrical configurations for the first wall, blanket, vacuum vessel and magnets are the same as in the previous model based on the outline design. It is expected that the designs for these components as well as the divertor cassette will go through several changes and the three-dimensional model developed here has to be updated again in 1995.

The output of the MCNP geometry plotting routine given in Fig. 10 shows a vertical cross section through the middle of the TF coil. The divertor cassette is divided into 6 zones representing the inner and outer legs, the inner and outer target plate regions, the middle part of the cassette and the central dome region. The model includes four cells representing the zones where the copper fins and support structure at the inner surfaces of the divertor cassettes are employed. Although these fins occupy a very small volume fraction of these cells, the model allows for including the additional radiation attenuation provided by these fins and their support structure in future calculations. A vertical cross section through the center of the divertor slots is shown in Fig. 11. Seven slots are shown in the figure. The conservative assumption that all the slots are open to the plasma chamber was made in the model. The model allows for including materials in

any of these slots to represent possible coolant plumping. Fig. 12 shows horizontal cross sections in the divertor region. In the cross section at $z = -5.2$ m, the slots in the central dome region and the horizontal slots behind the inner target plates are shown. At $z = -6$ m, one set of the slots behind the outer target plates along with the slots in the middle region of the cassette and the slots in the central dome region are shown. At $z = -6.3$ m, one set of the slots behind the outer target plates and part of one set of the slots in the middle region of the cassette are shown.

Although more divertor slots are used, streaming through the horizontal divertor ports is expected to be lower than in the outline design since these slots are not directed towards the horizontal ports. On the other hand, these slots can result in damage hot spots in the vacuum vessel behind the divertor cassettes. This effect needs to be assessed.

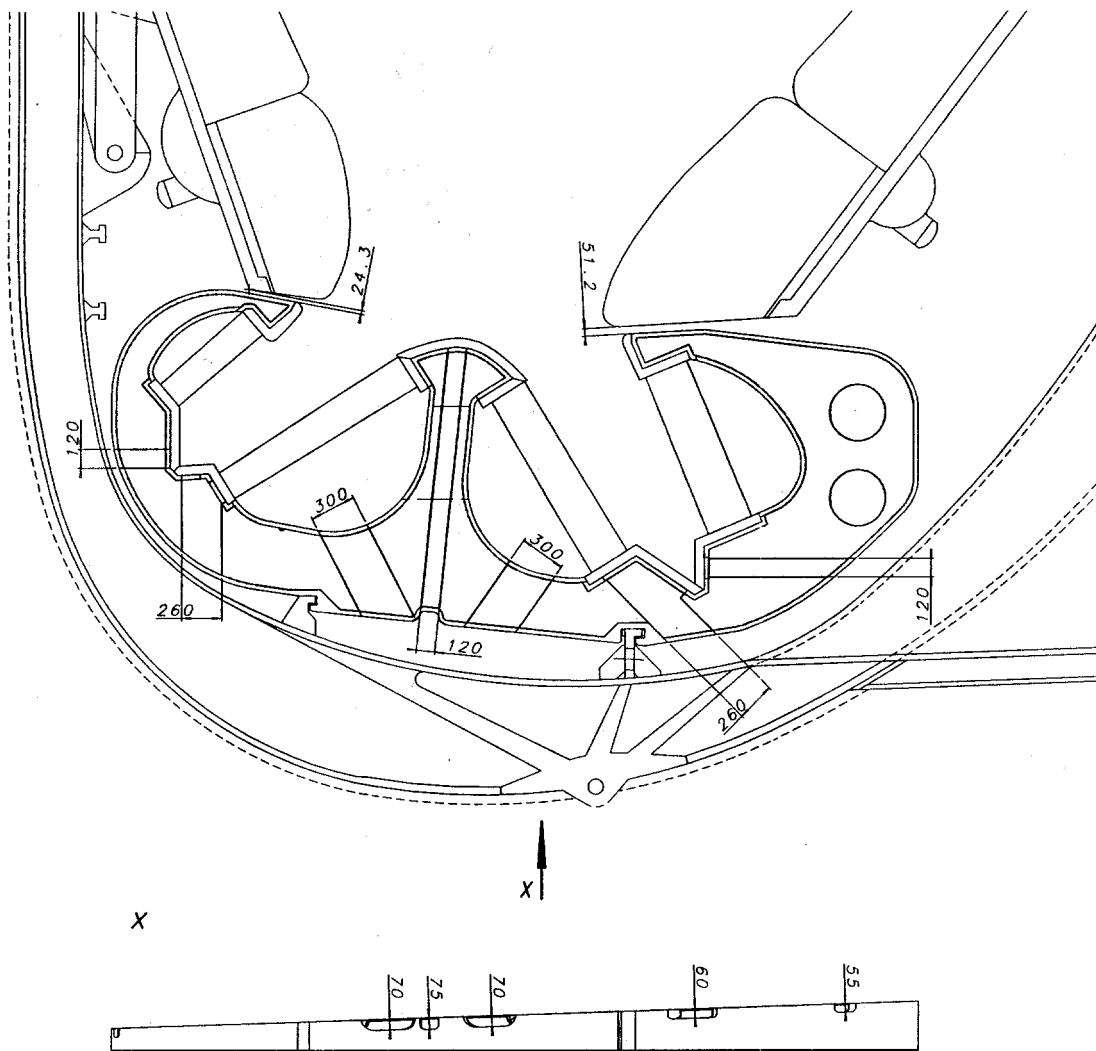


Fig. 9. Drawing of the most recent divertor cassette design.

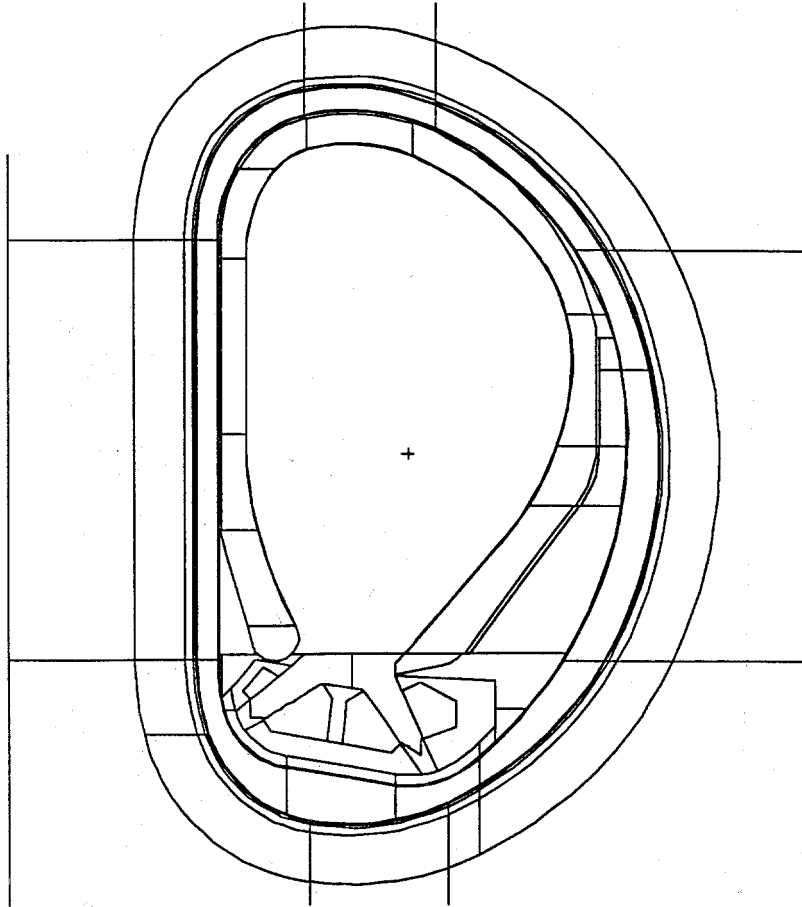


Fig. 10. Vertical cross section through a TF coil.

VII. FENDL Applications to ITER Neutronics and Shielding

The US home team participated in the IAEA Advisory Group Meeting on "Improved Evaluations and Integral Data Testing for FENDL" held in Garching on 12-16 September 1994. We generated a working cross section library based on the most recent international fusion evaluated nuclear data library (FENDL) [4]. The library includes all nuclear responses of interest for ITER design. The library was installed on the Garching JWS computer system in September 1994.

Calculations have been performed to determine the nuclear performance parameters for the first wall/blanket/vacuum vessel/magnet in the ITER outline design using data based on the FENDL/E-1.0 evaluation. Both the SS/water shielding blanket and the Li/V breeding blanket were considered. These one-dimensional calculations have been performed using the ONEDANT code

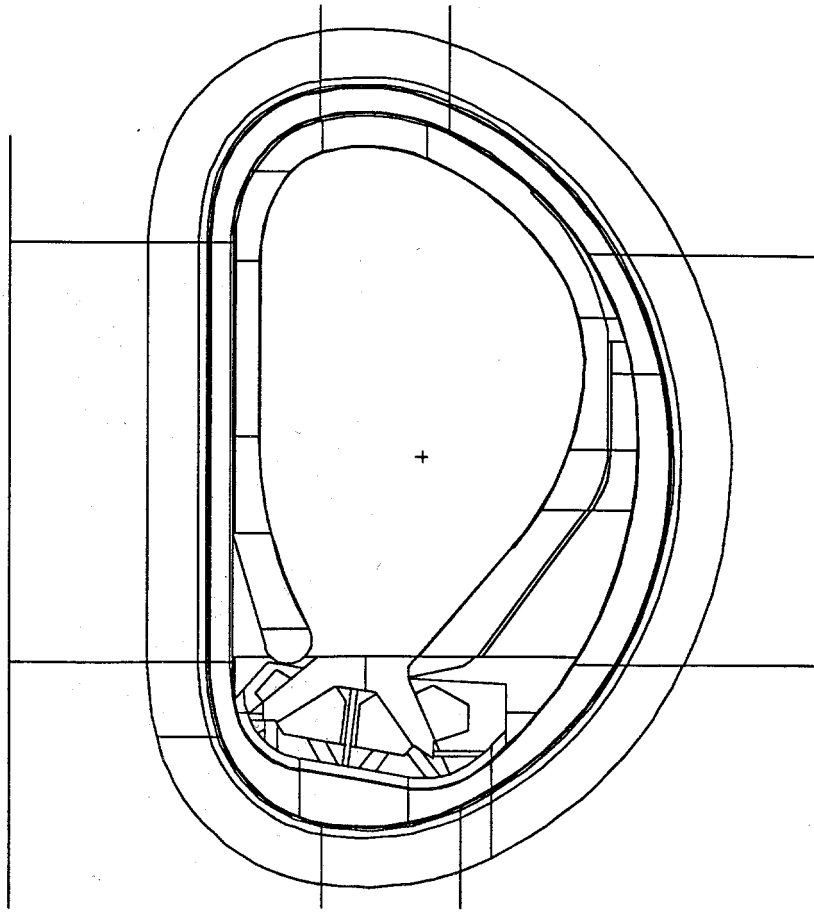
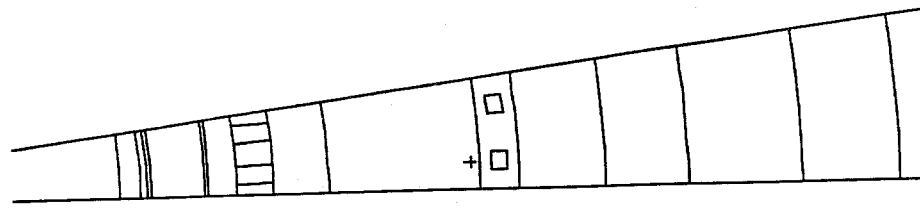
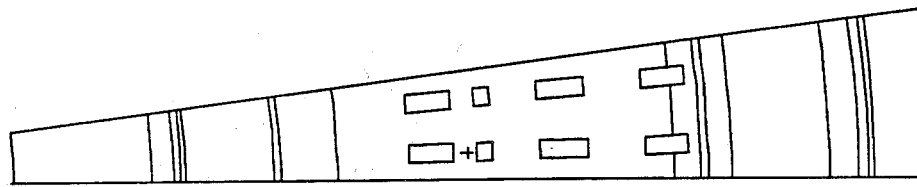


Fig. 11. Vertical cross section through divertor slots.

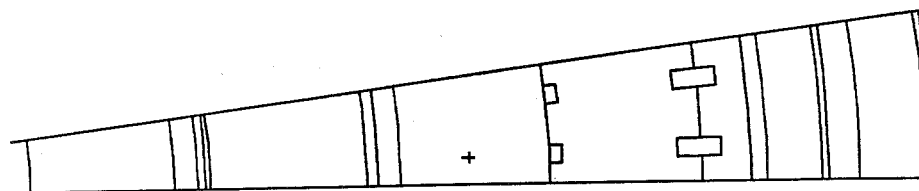
[7]. The results were compared to those obtained with previously used cross section libraries based on the ENDF/B-V evaluation [8]. The detailed neutronics and shielding results were presented in the IAEA Advisory Group Meeting on "Improved Evaluations and Integral Data Testing for FENDL" and provided to the ITER JCT. Differences in nuclear responses calculated with FENDL and ENDF/B-V using the same processing codes (NJOY/TRANSX) [9,10] are in general smaller than differences between results using different processing codes. Differences are, in general, smaller for the Li/V design than the SS/water design. The effect on nuclear heating of neglecting decay energy in the kerma factor is <10% with the largest effect in Cu and V. ENDF/B-V processed with MINX/AMPX/KAOS [11,12,13] gives larger heating than FENDL processed by NJOY/TRANSX. ENDF/B-V processed with MINX/AMPX/KAOS gives larger dpa than FENDL processed by NJOY/TRANSX except for the V FW. ENDF/B-V processed with



$Z = -5.2 \text{ m}$



$Z = -6 \text{ m}$



$Z = -6.3 \text{ m}$

Fig. 12. Horizontal cross sections in the divertor region.

Table 5. Peak Magnet Radiation Effects in the Inboard Leg

Evaluation Processing Codes	FENDL/E-1.0 NJOY TRANSX	ENDF/B-V NJOY TRANSX	ENDF/B-V MINX AMPX KAOS
Energy Groups Decay Energy	175n-42g No	30n-12g No	46n-21g Yes
End-of-life fast neutron fluence (n/cm ²)	1.46×10 ¹⁷	1.51×10 ¹⁷	1.99×10 ¹⁷
End-of-life insulator dose (Rads)	1.25×10 ⁸	1.32×10 ⁸	1.77×10 ⁸
End-of-life Cu dpa	9.44×10 ⁻⁵	9.96×10 ⁻⁵	1.29×10 ⁻⁴
Peak power density (mW/cm ³)	0.0296	0.0300	0.0435

MINX/AMPX/KAOS gives larger He production than FENDL processed by NJOY/TRANSX. ENDF/B-V processed with MINX/AMPX/KAOS and FENDL processed by NJOY/TRANSX give comparable tritium breeding results with <1% difference.

The peak magnet radiation effects in the inboard leg of the ITER outline design utilizing the shielding blanket are given in Table 5. The peak magnet radiation effects based on FENDL and ENDF/B-V using the same processing codes (NJOY/TRANSX) differ by less than 5% except for Cu dpa that differs by ~12%. The KAOS library based on ENDF/B-V gives higher peak magnet radiation effects than the FENDL library processed by NJOY. The difference is larger for gamma dominated effects (47% for power density and 42% for insulator dose) than for neutron effects (~36% for fast neutron fluence and Cu dpa). Different processing methods used need to be investigated and evaluated. Integral experiments for nuclear responses of interest to the designers will be useful to validate the processed nuclear response data.

VIII. ITER Design Relevant Computational Benchmarks

In order to help the JCT determine the codes and libraries to be used in neutronics, shielding and activation calculations, it was decided in the IAEA Advisory Group Meeting on "Improved Evaluations and Integral Data Testing for FENDL" [14] that calculational neutronics, shielding, and activation benchmarks based on the ITER design should be developed. Neutronics, shielding, and activation benchmark problems have been developed based on the shielding blanket design in the ITER outline design. The specifications along with the required flux files were placed in the

online system of the IAEA Nuclear Data Section and made available to the neutronics groups of the home teams.

The neutronics and shielding benchmark represents the reference steel/water shielding blanket design in the ITER outline design. The first wall is 14 mm thick consisting of 8 mm thick Be coating and 5 mm Cu attached to 1 mm thick SS. The shielding blanket is 526 mm thick with alternating layers of 316 SS and water. A double wall Inconel 625 vacuum vessel is used with single size water cooled 316 SS balls. The VV walls are 50 mm thick. A 50 mm thick back shield zone made of lead and boron carbide is used at the back of the VV. The total VV thickness is 455 mm in the inboard region and 619 mm in the outboard region. Figure 13 shows the radial build of calculational neutronics and the shielding benchmark. A 1-D toroidal cylindrical model with inboard and outboard regions modeled simultaneously is used. The model includes 54 zones divided into 573 mesh intervals. A maximum fine mesh interval width of 1 cm is used in the model except in plasma and void zones. A uniform 14.1 MeV isotropic neutron source in the plasma zone. The source in the plasma zone is normalized to 6.1×10^{17} n/cm²-s yielding inboard and outboard neutron wall loadings of 1 and 1.5 MW/m², respectively. The end-of-life results are based on a total ITER lifetime of 3 FPY (9.45×10^8 s).

To facilitate comparison of the design relevant parameters calculated by the different codes and libraries, a list of information that should be provided was compiled. This includes information on codes and data in addition to the calculation results as listed below.

1. Transport code used.
2. Angular quadrature order.
3. Legendre order of scattering.
4. Nuclear data evaluation used.
5. Nuclear data processing codes.
6. Energy group structure.
7. Weight function used to generate multigroup data.
8. Neutron and gamma fluxes in the first wall layers (Be, Cu, SS).
9. Peak neutron and gamma fluxes in vacuum vessel and magnet.
10. Nuclear heating (W/cm) in each of the non-void zones.
11. Power density (W/cm³) in the first wall layers (Be, Cu, SS).
12. Peak power density (W/cm³) in vacuum vessel and magnet.
13. End-of-life dpa in Cu and SS layers of first wall.
14. Peak end-of-life dpa in Inconel vacuum vessel.
15. End-of-life appm gas production (tritium, hydrogen, helium) in FW layers.
16. Peak end-of-life appm gas production in Inconel VV.
17. Peak end-of-life fast neutron fluence ($E > 0.1$ MeV) in magnet.
18. Peak end-of-life Cu dpa in magnet.
19. Peak end-of-life magnet insulator absorbed dose (eV/cm³).

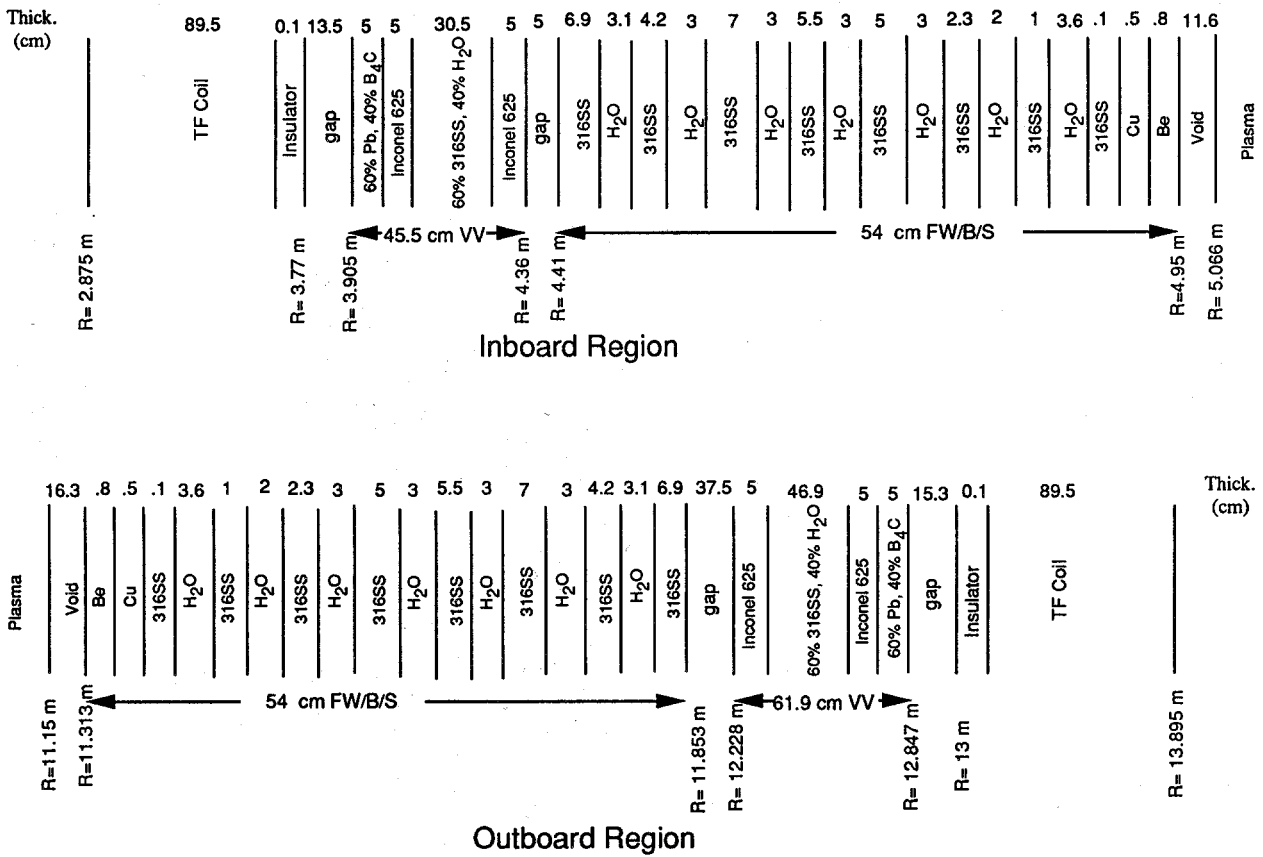


Fig. 13. Radial build of calculational neutronics and shielding benchmark.

The activation benchmark problem is similar to the neutronics and shielding benchmark described above except that the outboard magnet is not included. The model includes 51 zones divided into 468 intervals. The calculations are to be performed for two irradiation histories:

1. Continuous irradiation for 3 years (9.45×10^7 s).
2. Uniform pulsed operation with 94500 pulses each 1000 s wide with a dwell time of 1200 s between pulses.

In addition to the geometrical and material composition specifications, the neutron flux is provided at all fine mesh intervals in 175 energy group structure. The adjoint gamma flux is provided at all fine mesh intervals in 42 energy group structure to be used for dose rate calculations following shutdown.

The list of deliverables that will help the JCT decide on codes and libraries to be used for activation analysis includes information about codes and data and design relevant calculation results. The information to be reported is listed below.

1. Activation code used.
2. Activation data evaluation used.
3. Processing codes used to generate the activation library.
4. Energy group structure.
5. Weight function used to generate multigroup data.
6. Decay data library used.
7. Computing facility and CPU time used.
8. The specific activity (Bq/m^3) in the non-void zones at cooling times of 0, 1 hour, 1 day, 1 week, 1 month, 1 year, and 100 years after end of full reactor operation. The ten major contributing nuclides should be identified and their contributions provided.
9. The specific decay heat (W/m^3) in the non-void zones at cooling times of 0, 1 hour, 1 day, 1 week, 1 month, 1 year, and 100 years after end of full reactor operation. The ten major contributing nuclides should be identified and their contributions provided.
10. The energy spectra of decay gamma source in the non-void zones at the specified cooling times.
11. The biological dose rate (micro Sv/hr) at the back of the outboard shield at cooling times of 0, 1 hour, 1 day, 1 week, and 1 month after end of full reactor operation.

IX. Summary and Conclusions

A source subroutine was written to modify the Monte Carlo three-dimensional code MCNP to sample source neutrons from the source distribution in ITER plasma. A general ITER 3D model for MCNP was developed jointly by the US and EU home teams based on the ITER outline design. The model includes the first wall, blanket, divertor, vacuum vessel and TF magnets. The model includes also the pumping slots in the outer leg of the divertor. The poloidal distribution of the neutron wall loading in the different regions of ITER has been determined using MCNP. These calculations were performed for the ITER outline design. The results are valid for the current design since the neutron source profile, plasma shape and first wall configuration have not changed. The average neutron wall loading is 0.913 MW/m^2 for the nominal 1500 MW fusion power. The calculated average neutron wall loadings at the outboard and inboard first walls are 1.044 and 0.735 MW/m^2 , respectively. The peak outboard and inboard neutron wall loadings are 1.193 and 0.923 MW/m^2 , respectively.

Detailed 3D neutronics calculations have been performed for the divertor region in the outline design. The horizontal ducts are shielded from the plasma region by the approximately 80 cm thick lower end of the outboard blanket/shield and by the 40-60 cm thick outer divertor leg in front of the lower half of the duct. Based on this analysis, it is concluded that no additional divertor duct

shielding will be needed and the 20 cm thick duct wall along with the 11 cm thick mechanical structure will provide adequate protection for the TF coils against streaming radiation. In addition, parts of the TF coils behind the divertor cassettes are well shielded. Preliminary estimates of total nuclear heating in the TF coils were determined for both the SS/water and Li/V blankets of the ITER outline design. The results were based on the 3D calculations performed for the outline design. The total heating is less than 5 kW. The total heating is increased to 7 kW for the recent shielding blanket design presented in October at the design assessment meeting.

Detailed activation analysis has been performed for the first wall/blanket/vacuum vessel/magnet in the ITER outline design using different pulsed operation schedules. The calculations were performed for both the shielding blanket (SS/water) and the breeding blanket (Li/V) options. The activation code RACC modified for pulsing operation was used in the calculations. The detailed activation results were provided to the ITER JCT. This included the detailed spatial distribution of the radioactive inventory, afterheat and contact dose at different times following shutdown.

The nuclear performance parameters for the first wall/blanket/vacuum vessel/magnet in the ITER outline design using data based on the FENDL evaluation were determined and compared to those obtained with previously used cross section libraries based on the ENDF/B-V evaluation. The calculations were performed for both the shielding blanket (SS/water) and the breeding blanket (Li/V) options. The detailed neutronics and shielding results were provided to the ITER JCT. A working multigroup cross section library based on the most recent international fusion evaluated nuclear data library (FENDL) was generated. The library includes all nuclear responses of interest for the ITER design. The library was installed on the Garching JWS computer system in September. Neutronics, shielding, and activation benchmark problems have been developed based on the shielding blanket design in the ITER outline design. The specifications and required flux files were provided to the neutronics groups of the home teams. The results will help the JCT determine the codes and libraries to be used in neutronics, shielding and activation calculations.

The neutron source profile and plasma shape have not changed from the outline design. The major changes are in the divertor cassette design. In addition to the significant geometrical configuration changes, each divertor cassette includes 28 slots compared to only 5 slots in the outline design. The design presented at the end of October in the design assessment meeting was used as the basis for the updated general reactor 3D model. A complete updated general reactor model is provided to replace the model provided in March. Although more divertor slots are used, streaming through the horizontal divertor ports is expected to be lower than in the outline design since these slots are not directed towards the horizontal ports. On the other hand, these slots can result in damage hot spots in the vacuum vessel behind the divertor cassettes. This effect needs to

be investigated. It is assumed that the geometrical configurations for the first wall, blanket, vacuum vessel and magnets are the same as in the previous model based on the outline design. It is expected that the designs for these components will go through several changes and the 3D model has to be updated again in 1995.

References

- [1] P-H. Rebut, Detail of the ITER outline design report, ITER Report, ITER-TAC-4-06, Vols. 1-3, 10 January 1994.
- [2] J. Briesmeister (Editor), MCNP, a general Monte Carlo code for neutron and photon transport, version 3A, LA-7396-M, Rev. 2, Los Alamos National Laboratory (September 1986, revised April 1991) and Summary of MCNP Commands, Version 4.2, LANL Draft (September 1991).
- [3] H. Attaya, "1994 Summary Report for ITER Design Task D4, Part B: Activation," Argonne National Laboratory Report, ANL/FPP/TM-276 (January 1995).
- [4] IAEA Specialists Meeting on the Fusion Evaluated Nuclear Data Library (FENDL), Vienna, Austria, May 1989; Summary Report Edited by V. Goulo and Published as IAEA Nuclear Data Section Report INDC(NDS)-223/GF (1989).
- [5] J-C. Nimal and T. Vergnaud, "TRIPOLI-3 Code de Monte Carlo Tridimensionnel Polycinetique", CEA/DRN/DMT/SERMA Saclay, France, 1993.
- [6] J-Ch. Sublet, "ITER Neutronics Analysis, Neutron Wall Loading Distribution and Components Spectral Data," UKAEA/NID-4d/SEP1-1/2(94), UKAEA, Culham, UK (August 1994).
- [7] R.D. O'Dell et al., "User's manual for ONEDANT: a code package for one-dimensional, diffusion-accelerated, neutral particle transport," Los Alamos National Laboratory Report, LA-9184-M (1989).
- [8] R. Kinsey, comp., "ENDF/B Summary Documentation," National Nuclear Data Center, Brookhaven National Laboratory Report BNL-NCS-17541 (ENDF-201), 3rd Ed., ENDF/B-V (1979).
- [9] R. MacFarlane et al., "NJOY 91.38, A Code System for Producing Pointwise and Multigroup Neutron and Photon Cross Sections from ENDF/B Evaluated Nuclear Data," PSR-171, Radiation Shielding Information Center, Oak Ridge National Laboratory (July 1992).

- [10] R. MacFarlane, "TRANSX 2: A Code for Interfacing MATX Cross Section Libraries to Nuclear Transport Codes," Los Alamos National Laboratory Report, LA-12312-MS (July 1992).
- [11] C. Weisbin et al., "MINX, A Multigroup Interpretation of Nuclear Cross Sections, Los Alamos National Laboratory Report, LA-6486-MS (1976).
- [12] N. Greene et al., "AMPX: A Modular Code System for Generating Coupled Multigroup Neutron-Gamma Libraries from ENDF/B," Oak Ridge National Laboratory Report, ORNL/TM-3706 (1976).
- [13] Y. Farawila, Y. Gohar and C. Maynard, "KAOS/LIB-V: A Library of Nuclear Response Functions Generated by KAOS-V Code from ENDF/B-V," Argonne National Laboratory Report ANL/FPP/TM-241 (April 1989).
- [14] IAEA Advisory Group Meeting on "Improved Evaluations and Integral Data Testing for FENDL", Garching, Germany, September 1994; Summary Report Prepared by S. Ganesan and Published as IAEA Nuclear Data Section Report INDC(NDS)-312 (1994).